JOURNAL OF MATERIALS SCIENCE 13 (1978) 611–619

Tensile creep and high-temperature fracture in a Li_2O-Al_2O_3-$4SiO_2$ glass-ceramic

S. E. BOLD, G. W. GROVES
Department of Metallurgy and Science of Materials, University of Oxford, Oxford, UK

A glass of composition $Li_2O-Al_2O_3-4SiO_2$ with TiO_2 as nucleating agent was heat-treated to produce either β-quartz or β-spodumene crystal phases and the tensile creep properties of the two structures were investigated. Both exhibited substantial creep ductility and the strain rate $\dot{\epsilon}$ in both could be expressed by an equation of the form:

$$\dot{\epsilon} = A\sigma^n \exp(-\Delta H/RT),$$

where σ is the tensile stress and T the temperature. Within experimental error the stress exponent n and activation energy ΔH were the same for β-quartz and β-spodumene ($n = 1.4$ and $\Delta H = 695\,kJ\,mol^{-1}$) but the constant A was approximately 10^3 times larger for β-quartz than for β-spodumene. This more rapid creep in β-quartz is attributed to its much finer grain size. The mechanism of deformation is believed to be grain-boundary sliding accommodated by grain-boundary diffusion. This belief is supported by observations of the microstructure of the β-spodumene after tensile strains as large as 30%. Creep tests terminated in brittle fracture when an intergranular crack growing slowly from a surface defect reached a critical size. It is interesting to note that this phenomenon of subcritical crack growth occurred in the absence of any detectable intergranular glass phase.

1. Introduction

A number of fine-grained ceramics such as silicon nitride, silicon carbide and certain glass-ceramics have good thermal shock resistance and low temperature strength. The high temperature mechanical properties of these materials are therefore of great interest from the point of view of structural applications at high temperatures. Previous work has indicated that the presence of a glass phase at the grain-boundaries is of great importance in these materials. Thus Kossowsky *et al.* [1] investigated the tensile creep of hot-pressed silicon nitride and believed it to be controlled by the viscous flow of a grain-boundary glass phase. Dislocations within the grains were not believed to play a significant part although Salah ud Din and Nicholson [2] suggested that a stress exponent exceeding unity, which they observed in a study of creep in bending of hot-pressed silicon nitride, could be explained by some degree of plastic deformation within grains. The tensile and compressive creep of two lithium zinc silicate glass-ceramics containing 20% residual glass phase was studied by Morrell and Ashbee [3]. They concluded that deformation was controlled by the glass phase in which void formation occurred, enhancing the creep rate, promoting low strain fracture and giving rise to a stress exponent greater than unity. In a recent review of creep in glass-ceramics, James and Ashbee [4] proposed a deformation model of dilatancy and stress-induced crystal dissolution and reprecipitation for lithium disilicate and fluorophlogopite glass-ceramics having a high glass content. In a study of torsional creep in glass-ceramics including $Li_2O-Al_2O_3-SiO_2$ materials, Heuse and Partridge [5] proposed a creep mechanism of viscous flow within the glass phase. They also reported an increasing creep resistance with increasing heat treatment temperature in a $Li_2O-Al_2O_3-SiO_2$ glass-ceramic.

Barry *et al.* [6] studied the resistance to creep in bending of a cordierite glass-ceramic as a func-

tion of various oxide additions to a relatively pure $MgO-Al_2O_3-SiO_2$ base. Additions of K_2O or CaO were particularly effective in reducing the creep resistance. A creep resistant composition was studied in more detail by tensile creep testing. Tensile strains in excess of 25% were obtained and a stress exponent of 2.1 was found. Deformation by a diffusion mechanism was proposed, and microstructural examination showed that voids had developed during creep.

A comparison of the creep in bending of various glass-ceramics with Li_2O, Al_2O_3 and SiO_2 as the major components was made by Barry *et al.* [7]. Two commercial glass-ceramics were found to have inferior creep properties to an experimental material of composition $Li_2O-Al_2O_3-4SiO_2$, made with relatively pure raw materials. A commercial material in which there was evidence of a continuous grain-boundary glass phase gave particularly rapid creep and fractured at a strain of less than 2% at the tensile surface. No glass phase could be detected in the relatively creep-resistant experimental material.

In the work reported in the present paper a $Li_2O-Al_2O_3-4SiO_2$ glass-ceramic similar to that reported on by Barry *et al.* [7] was used for a detailed study of the tensile creep properties of two microstructures produced by different heat treatments.

2. Experimental

2.1. Preparation of material

The glass was made up with the assistance of Dr T. I. Barry at the National Physical Laboratory. The constituents, with the manufacturers claimed purities were laboratory grade lithium carbonate (> 99%), Cera alumina (99.8%), Thermal Syndicate crushed quartz (99.8%) and Laporte titanium dioxide (99.5%). The composition used was $Li_2O-Al_2O_3-4SiO_2$ with 3 mol% TiO_2 added as a nucleating agent. A melting procedure was developed with avoided inhomogeneities in the glass.

After mixing the powers in a rolling mill, a 0.5 Kg batch was melted at 1550° C for 4 h and poured into water. The fragmented glass was remelted and held overnight at 1550° C to allow bubbles to escape. The further removal of bubbles involved raising the temperature to 1600° C for 2 h and stirring with a fused silica rod. Finally, any small bubbles remaining were redissolved by lowering the temperature to 1550° C. The liquid was poured into a graphite-coated steel mould, pre-heated to 400° C. The glass bar was then annealed at 720° C to relax internal stresses. In crystallizing the glass, the rate of heating was controlled so that the decrease in viscosity of the glass due to a rise in temperature was compensated for by an increase in viscosity due to crystallization. The heat-treatments used to produce β-quartz or β-spodumene were:

β-quartz

0 → 718	718 → 760	760 → 1000° C
2 h 20 min	3 h	1 h 10 min

β-spodumene

0 → 718	705 → 755	755 → 1230 or 1200° C
2 h 20 min	3 h 20 min	2 h 20 min

held 1230 or 1200° C
4 h

2.2. Creep testing

Bars of dimension 3 mm x 3 mm x 240 mm were cut out with a diamond saw and subjected to a constant tensile load on a Denison creep machine. A small furnace providing a hot zone of approximately 15 mm was attached to the creep machine and the ends of the bar were glued into water-cooled grips outside the furnace, which were threaded into universal joints. The extension of the bar was measured by two LVDT's mounted on either side of the specimen so that bending of the specimen would be detectable as a difference in the LVDT readings.

Because the temperature profile of the furnace is not a perfect step function it is necessary to take account of the contribution of the entire length of the specimen to the measured extension. The strain rate is assumed to be governed by a constant activation energy H. The strain rate at the maximum temperature of the furnace T_m is then given by;

$$\dot{\epsilon}_m = \frac{1}{l_{eff}} \frac{dl}{dt} \tag{1}$$

where l is the length of the specimen and l_{eff} the "effective gauge length", given by [8]:

$$l_{eff} = \int_0^l \frac{\exp \Delta H/RT_m}{\exp \Delta H/RT} dx \tag{2}$$

In Equation 2 T is the temperature at a distance x along the specimen. Experimentally, T is determined as a function of x by passing a thermocouple along the specimen, and the integration to obtain l_{eff} is then performed numerically. Initially, the

activation energy determined for similar material from bending creep tests [7] was used to estimate ΔH. From the results of temperature change tests an experimental value of ΔH is then derived and used to correct the effective gauge lengths. The value of ΔH can then be given a further small adjustment to give consistence between the ΔH used in Equation 2 and that obtained from temperature-change tests.

2.3. Electron microscopy

The procedure used to prepare specimens for transmission electron microscopy (TEM) was that of mechanical polishing followed by ion beam thinning, as described by Clinton [9]. Specimens were examined at 100 kV and some difficulty was caused by electron damage which led to a fairly rapid loss of crystallinity followed by void formation under a beam of normal strength. However, with care adequate diffraction patterns and micrographs could be obtained.

3. Results

3.1. Microstructures

3.1.1. β-quartz solid solution

The β-quartz phase, identified as such from both electron and X-ray diffraction patterns, is shown in Fig. 1. The structure may be regarded as a solid solution between the β-quartz form of silica [10] and the stuffed derivative of β-quartz of composition $Li_2O-Al_2O_3-2SiO_2$, β-eucryptite. The lattice is hexagonal; its lattice parameters were found to be $a = 0.517$ nm, $c = 0.539$ nm. The variation of the lattice parameters of this solid solution with composition has been determined by Nakagawa and Izumitani [11].

Neither the electron nor X-ray diffraction patterns gave evidence of the presence of a glass phase. However the rounded appearance of some grains and the unexplained shadowy contrast apparently outlining grains (Fig. 1) leave the suspicion that a small amount of intergranular glass phase may be present.

The grain size was measured by drawing random lines and measuring the intercept length for 100 individual grains which were visible in diffraction contrast. This method is subject to some systematic error of overestimation in that the foil thickness is not negligible compared to the grain size, so that there is a projection effect, such that the maximum grain width is measured. The mean intercept length of 0.145 μm is therefore estimated to be subject to an error +0.014 μm, −0.035 μm.

The small particles visible in Fig. 1 are believed to be TiO_2, although there was no direct evidence of this from the electron diffraction pattern.

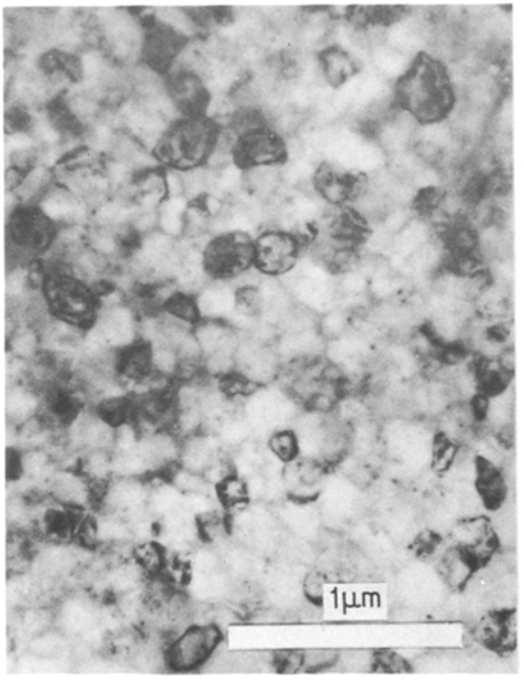

Figure 1 The microstructure of the β-quartz solid solution material.

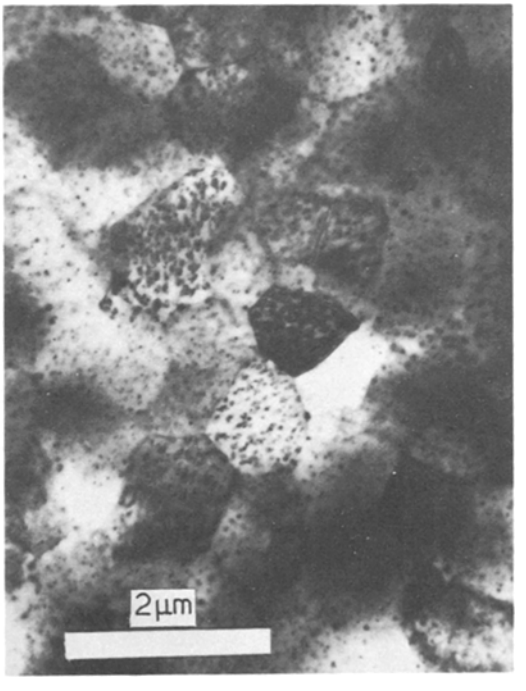

Figure 2 The microstructure of the β-spodumene material after heat treatment to 1200° C.

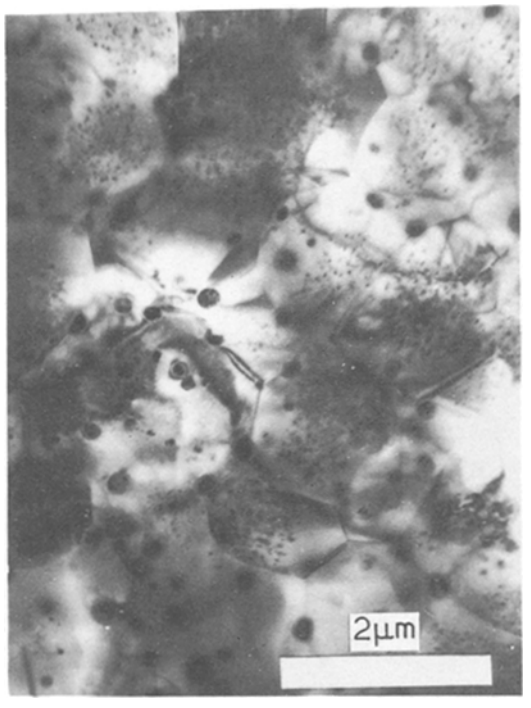

Figure 3 The microstructure of the β-spodumene material after heat treatment to 1230° C.

3.1.2. β-spodumene

After heat treatment to 1200 or 1230° C the presence of β-spodumene [12] was confirmed by X-ray and electron diffraction. In the 1200° C material (Fig. 2) the precipitate, presumed to be TiO_2 (again without direct electron diffraction evidence) is uniformly distributed whereas in the 1230° C material (Fig. 3) some grain-boundary motion appears to have occurred, leading to the formation of coarse grain-boundary precipitates, by the coalescence or rapid Ostwald ripening of small precipitates intersected by the moving grain-boundary. Specimens were extensively tilted in the electron microscope to vary the diffraction contrast, but no sign of a glass phase could be detected, and grain-boundary triple points always appeared perfectly sharp. The grain size of the 1230° C material was measured as accurately as possible by the line intercept method as 1.00 ± 0.10 μm, the random error being estimated according to the treatment of Hilliard [13].

The microstructures observed here are in good agreement with those in similar material reported by Barry *et al.* [7].

3.2. Creep data

Fig. 4 shows typical extension–time curves. A very small period of primary creep is followed by an extensive period of constant elongation rate. At long times the extension rate shows some decrease. The long linear stage of creep was very favourable for determining the stress and temperature dependence of the creep rate in the secondary state, by making load and temperature changes respectively. Stress changes were made above and below a mean value, which was repeated at intervals throughout the experiment to check the reproducibility of the results and reveal any progressive change in strain rate. This check did reveal an overall drop in the strain rate of the β-quartz material which was accounted for by the microstructural changes described in the following section. When either stress or temperature was changed there was a period of transient creep before the new constant creep rate was established. The extent of this was clear and it could usually be excluded from

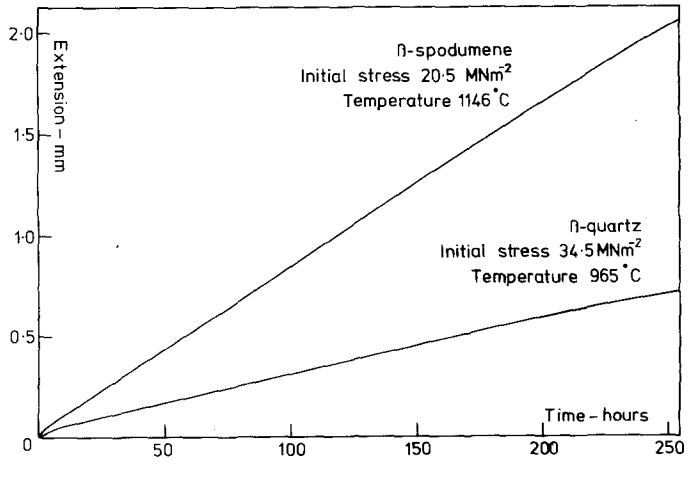

Figure 4 Typical extension versus time curves.

measurement without difficulty. The most difficult case arises when the stress is changed from a high to a low value, since in this case even a small viscoelastic recovery of the specimen can subtract significantly from the small secondary creep rate at the low stress. In such cases a prolonged period at the low stress was used to establish the creep rate.

The results of stress change tests for the β-quartz and β-spodumene (1230° C) material are shown in Figs. 5 and 6 respectively. They show that at a constant temperature the strain rate can be expressed as;

$$\dot{\epsilon} = A\sigma^n \qquad (3)$$

where A is a constant, different for β-quartz and

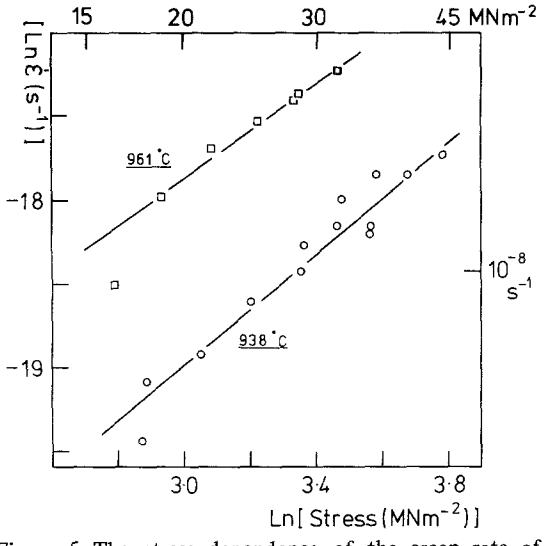

Figure 5 The stress dependence of the creep rate of β-quartz solid solution – data from stress-change tests on two test-pieces.

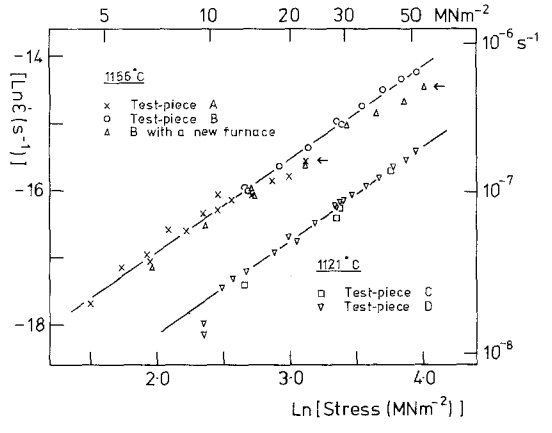

Figure 6 The stress-dependence of the creep rate of β-spodumene – data from stress-change tests. The arrowed points are the measurements made immediately prior to the fracture of the specimen.

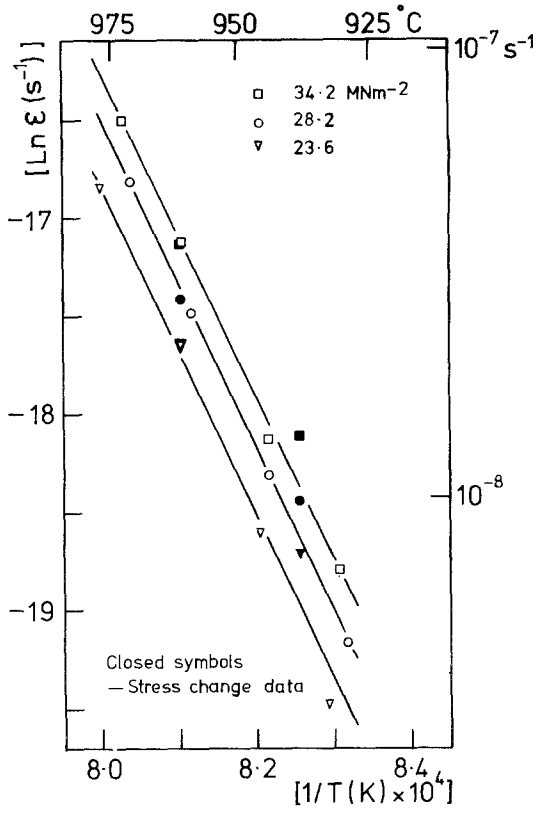

Figure 7 The temperature-dependence of the creep rate of β-quartz solid solution – data from temperature-change tests on two test pieces. Data from the stress-change tests are also plotted, as solid symbols.

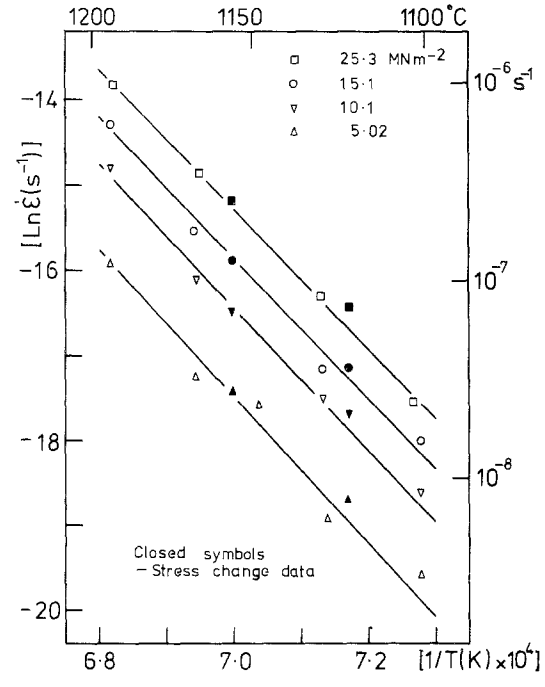

Figure 8 The temperature-dependence of the creep rate of β-spodumene – data from stress-change tests are also plotted, as solid symbols.

β-spodume and the stress exponent $n = 1.4 \pm 0.2$ for both materials. The result for β-spodumene alone can be expressed wih more precision as $n = 1.4 \pm 0.1$ in the stress range 5 to 50 MN m^{-2}. Figs. 7 and 8 show the results of temperature change tests for β-quartz and β-spodumene (1230° C) respectively. The secondary strain rate can evidently be expressed as;

$$\dot{\epsilon} = B\sigma^n \exp(-\Delta H/RT) \quad (4)$$

The activation energy ΔH does not vary significantly with stress and has the value 691 ± 9 kJ mol^{-1} for β-quartz and 698 ± 14 kJ mol^{-1} for β-spodumene. The activation energy is therefore the same, within experimental error, for both materials. Secondary creep in both materials can therefore be described by similar equations:

for β-quartz, $\dot{\epsilon} = B_q \sigma^{1.4} \exp(-\Delta H/RT)$ (5)

for β-spodumene, $\dot{\epsilon} = B_s \sigma^{1.4} \exp(-\Delta H/RT)$ (6)

where $\Delta H = 695$ kJ mol^{-1}. Comparison of the absolute values of the creep rates in the two materials gives, for $\dot{\epsilon}$ in sec^{-1} and σ in MN m^{-2};

$$B_q = 6.30 \times 10^{19} \quad (7)$$

$$B_s = 7.45 \times 10^{16} \quad (8)$$

The β-quartz would therefore creep about 850 times as fast as the β-spodumene under the same conditions.

3.3. Microstructures after creep

In the creep testing of the β-quartz the strain rates were observed to decrease significantly after some time. At the end of a creep test a specimen examined in the electron microscope showed from its diffraction pattern that some conversion to β-spodumene had occurred. A relatively large β-spodumene grain can be seen in strong contrast in Fig. 9 which also shows that there has been a coarsening of the TiO_2 particles.

The β-spodumene (1230° C) material after creep showed no significant change in microstructure other than the occasional appearance of voids at grain boundaries (Fig. 10). These were unmistakable but rather uncommon – typically only one in four of areas similar to that shown in Fig. 10 would contain a void. They appear to lie mainly on grain boundaries perpendicular to the stress and to have their smallest dimension in the direction of the stress. The β-spodumene (1200° C) material

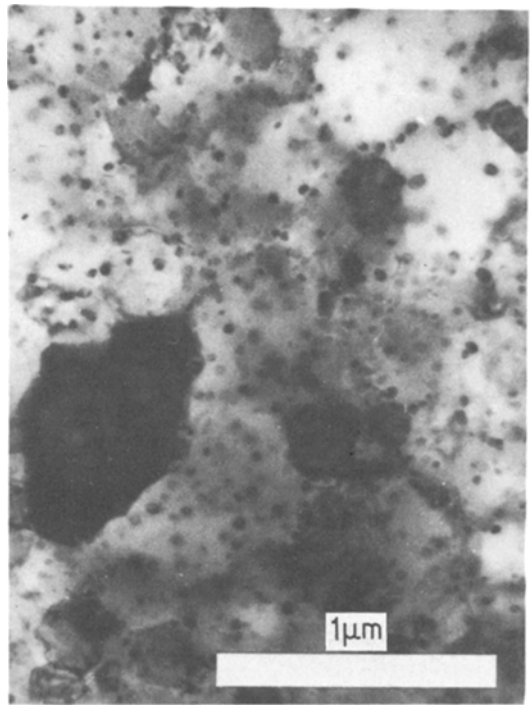

Figure 9 The microstructure of the β-quartz solid solution after a creep extension of 3.5%.

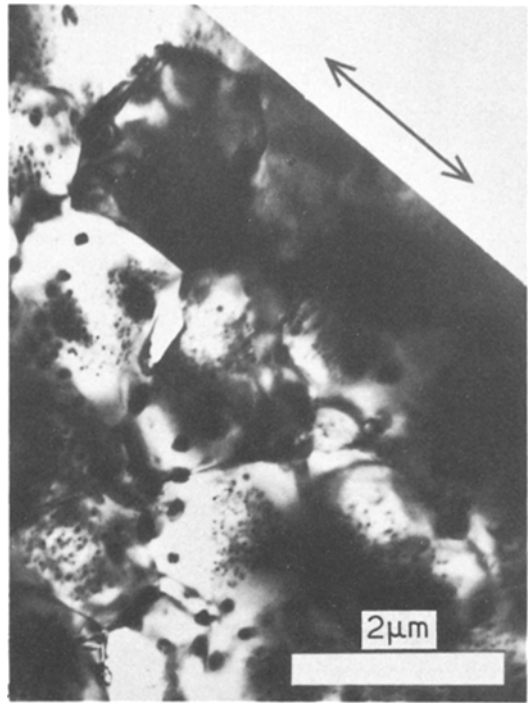

Figure 10 The microstructure of the β-spodumene material (heat treated at 1230° C) after a creep elongation of 14%. The stress axis is in the plane of the micrograph in the direction indicated by the arrows.

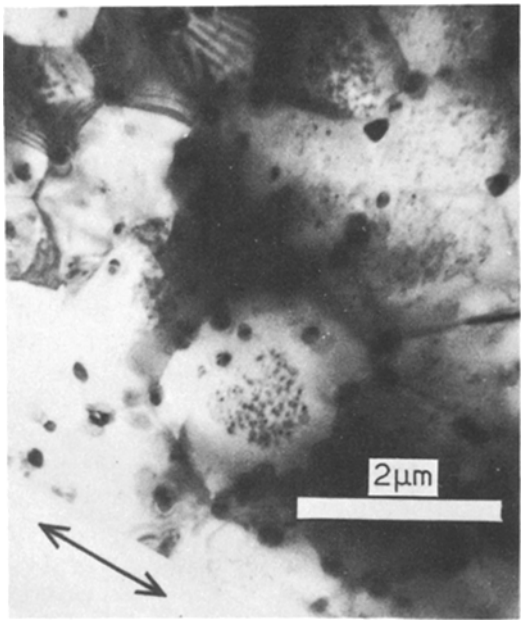

Figure 11 The microstructure of the β-spodumene material (heat treated at 1200° C) after a creep elongation of 30%. The stress axis is in the plane of the micrograph in the direction shown by the arrows.

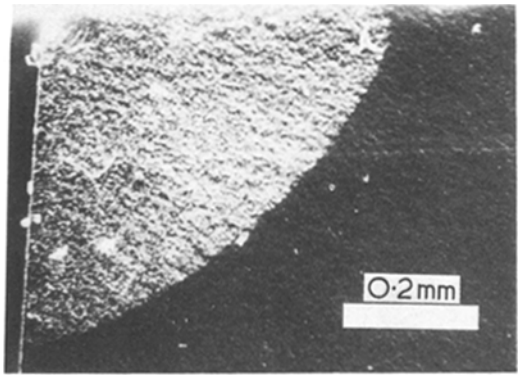

Figure 12 Macroscopic appearance of the fracture surface of a β-spodumene specimen.

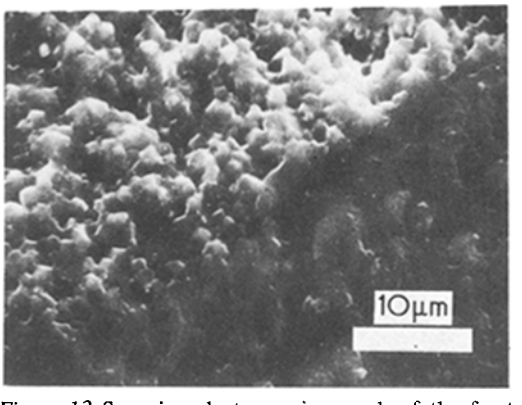

Figure 13 Scanning electron micrograph of the fracture surface of a β-spodumene specimen (angle betwen beam and surface normal = 25°). The borderline between the two regions of fracture is shown.

was not creep tested extensively enough to give quantitative creep data for it, but the appearance of this material after a total creep strain of 30% undergone at various temperatures below 1200° C is shown in Fig. 11. It is noticeable that even at this large strain there is no detectable elongation of the grains in the direction of the stress, and no dislocations are present. Grain-boundary migration leading to zones denuded of TiO_2 and coarse grain-boundary precipitates of TiO_2 has evidently occurred.

3.4. Fracture

Specimens failed by a brittle fracture which occurred without warning and with no prior acceleration of the creep rate. In the case of the β-spodumene specimens the fracture surfaces showed a region, visible to the naked eye, of different reflectivity, at a corner or edge of the fracture surface (Fig. 12). Viewed in the scanning electron microscope this region was seen to be very rough, on the scale of the grain size (Fig. 13). The division between this area and the remaining, relatively smooth area of the fracture surface, was sharp. The implication is that a crack nucleated at an early stage at some surface flaw, and grew slowly during the creep test until a critical size was reached, at which point catastrophic transgranular propagation occurred. From the equation;

$$K = \frac{2\sigma a^{1/2}}{\pi^{1/2}} \qquad (9)$$

for the stress intensity factor K due to a circular crack of radius a under a tensile stress σ, the critical stress intensity factor for catastrophic crack propagation in β-spodumene at 1150 to 1200° C was estimated to be 0.6 MN m$^{-3/2}$.

In the case of the β-quartz material the origin of the fracture was not evident.

4. Discussion

The glass-ceramic studied here is notable for its rather simple creep behaviour in both the β-quartz and β-spodumene forms. The creep curves show extensive periods of constant strain rate, governed by a stress-independent activation energy of 695 kJ mol^{-1}. This value is somewhat lower than that of 940 kJ mol^{-1} derived by Barry *et al.* from

the creep in bending of a similar material [7]. The exact reason for this discrepancy is not clear but in general tensile creep would be expected to yield a more definitive value than bending creep in which the strain is highly inhomogeneous. The activation energy of 695 kJ mol^{-1}, although high, is similar in magnitude to that of 714 kJ mol^{-1} governing the viscosity of pure silica glass [14].

The equality of the activation energies and stress exponents for β-quartz and β-spodumene suggests that a very similar deformation mechanism operates in both cases. The similarity of the grain structures of the β-spodumene before and after large creep strains, the absence of dislocations within the grains and the stress exponent of 1.4 are all reminiscent of the behaviour of superplastic materials [15]. The observations suggest a deformation mechanism of grain-boundary sliding accommodated by a diffusion process in the manner proposed for example by Ashby and Verall [16].

Whether the accommodating diffusion process is grain-boundary diffusion, as in Coble creep [17], or diffusion through the grains, as in Nabarro–Herring creep [18] could best be determined by finding whether the creep rate depended on grain size d as d^{-3} (Coble creep) or d^{-2} (Nabarro–Herring creep). In fact we have only a comparison between two different phases of different grain sizes. If it is assumed that the difference between the creep rates of β-quartz and β-spodumene is determined dominantly by the large grain size difference, then allowing for the estimated errors in measuring the grain sizes, the grain size exponent should lie in the range 2.9 to 3.9. This gives some tentative support to the grain-boundary diffusion mechanism.

For the Coble creep mechanism, or the related mechanism of grain-boundary sliding with grain-switching events accommodated by grain-boundary diffusion as proposed by Ashby and Verall [16] the stress exponent should be unity. In fact the observed stress exponent for our material is 1.4. This is consistent with the findings of stress exponents which are small but greater than unity in other fine-grained ceramics – between 1.4 and 2.2 for various glass-ceramics [5], 2.1 for a cordierite glass-ceramic [6] and 1.7 for hot-pressed silicon nitride [2] for example. The value of 1.4 is also typical of the stress exponents found is superplastic alloys [15], although in this case in a considerably higher range of strain rate than is normally covered in creep experiments. In our case the explanation of an increased stress exponent as due to a contribution from dislocation creep appears improbable, especially for the very fine-grained β-quartz material. The effect of a constant threshold stress, or internal stress σ_i which subtracts from the applied stress so that the strain rate is proportional to $(\sigma - \sigma_i)$ could not in our case account for the results on β-spodumene at 1156° C, which cover a very wide range of stress (Fig. 6). It is possible that the interface reactions in which vacancies are generated or absorbed in a grain-boundary are sluggish enough to have an influence on the overall rate of the deformation process. A complicated form of stress dependence might arise in this way [16].

Void formation during creep appears qualitatively similar in our material to that observed in cordierite glass-ceramics [6] or in silicon nitride [1, 2] although in our case the density of voids is relatively low (certainly too low to accommodate significantly the grain-boundary sliding or to significantly enhance the creep rate). It may be that the growth and linkage of intergranular voids in the region of high strain concentration near the tip of a crack accounts for slow subcritical crack growth in the manner suggested by Lange for the subcritical growth of cracks in silicon nitride [19]. The very rough fracture surface of the slow crack is consistent with such a mechanism (Fig. 12).

It is worth emphasizing that in our material slow crack growth occurs in the absence of any detectable glass phase. The viscosity of the glass phase present in silicon nitride has been proposed to be of prime importance in determining the velocity of subcritical crack growth [19]. The present work suggests that even if the amount of glass phase in this and similar materials is reduced below the level of detection, the phenomenon of subcritical crack growth will still occur.

5. Conclusions

The tensile creep characteristics of a Li_2O–Al_2O_3–$4SiO_2$ glass-ceramic have been established for two microstructures, a 0.14 μm grain size β-quartz solid solution and a 1.0 μm grain size β-spodumene. In both the strain rate is governed by an activation energy of 695 kJ mol^{-1} and the stress dependence of the strain rate is the same for both, the stress exponent being 1.4. From observations of the microstructures after large creep strain and from a comparison of the rates of creep

of the two microstructures it is concluded that the basic mechanism of creep deformation is grain-boundary sliding accommodated by grain-boundary diffusion. Despite the attainment of large tensile creep strains amounting in some cases to several tens of per cent elongation the ultimate fracture is brittle in character. In the β-spodumene the slow intergranular growth of a subcritical crack leads up to the final brittle fracture, even though the microstructure contains no detectable intergranular glass phase.

Acknowledgements

Thanks are due to Dr T. I. Barry and Dr R. Morrell for helpful discussions and to the above together with Mr L. A. Lay and Mr J. Cox of the National Physical Laboratory for their help in producing the material used in this work. Financial assistance from the National Physical Laboratory and the support of an S.R.C. CASE studentship are also acknowledged.

References

1. RAM KOSSOWSKY, D. G. MILLER and E. S. DIAZ, *J. Mater. Sci.* **10** (1975) 983.
2. SALUH UD DIN and P. S. NICHOLSON, *ibid* **10** (1975) 1375.
3. R. MORRELL and K. H. G. ASHBEE, *ibid* 8 (1973) 1253.
4. K. JAMES and K. H. G. ASHBEE, *Prog. Mater. Sci.* **21** (1975) 1.
5. E. M. HEUSE and G. PARTRIDGE, *J. Mater. Sci.* 9 (1974) 1255.
6. T. I. BARRY, L. A. LAY and R. MORRELL, *Proc. Brit. Ceram. Soc.* **25** (1975) 67.
7. T. I. BARRY, D. J. CLINTON and L. A. LAY, Proceedings of the 6th International Materials Symposium "Ceramic Microstructures" edited by R. M. Fulrath and J. A. Pask (West View Press, Boulder Colorado, 1977) p. 479.
8. D. J. GOOCH and G. W. GROVES, *J. Mater. Sci.* 8 (1973) 1238.
9. D. J. CLINTON, *Micron* 3 (1972) 358.
10. W. A. DEER, R. A. HOWIE and J. ZUSSMAN, "Rock Forming Minerals" Vol. 4 (J. Wiley, New York, 1963) p. 182.
11. K. NAKAGAWA and T. IZUMITANI, *J. Non-Cryst. Solids* 7 (1972) 168.
12. CHI-TANG LI and D. R. PEACOR, *Zeit.f.Krist* **126** (1968) 46.
13. J. E. HILLIARD, "Recrystallization, Grain Growth and Textures" (American Society for Metals, Metals Park, Ohio, 1963) p. 267.
14. R. BRÜCKNER, *J. Non-Cryst. Solids* 5 (1971) 177.
15. J. W. EDINGTON, K. N. MELTON and C. P. CUTLER, *Prog. Mater. Sci.* **21** (1976) 61.
16. M. F. ASHBY and R. A. VERRALL, *Acta Met.* **21** (1973) 149.
17. R. L. COBLE, *J. Appl. Phys.* **34** (1963) 1679.
18. C. HERRING, *ibid* **21** (1950) 437.
19. F. F. LANGE, *J. Amer. Ceram. Soc.* 57 (1974) 84.

Received 30 May and accepted 8 July 1977.